

Design and Manufacturing of a Hexapattern Frequency Selective Surface Absorber for Aerospace Stealth Application

Priyanka¹, Subrat Mohanty¹, Prashant S Alegaonkar^{1,*}, Himangshu B Baskey²

¹*Department of Physics, School of Basic Sciences, Central University of Punjab, Bathinda, Punjab 151401, India*

²*Stealth and Camouflage Division, Defence Material Store R and D Establishment, DRDO, Kanpur, UP208013, India*

Supporting Information

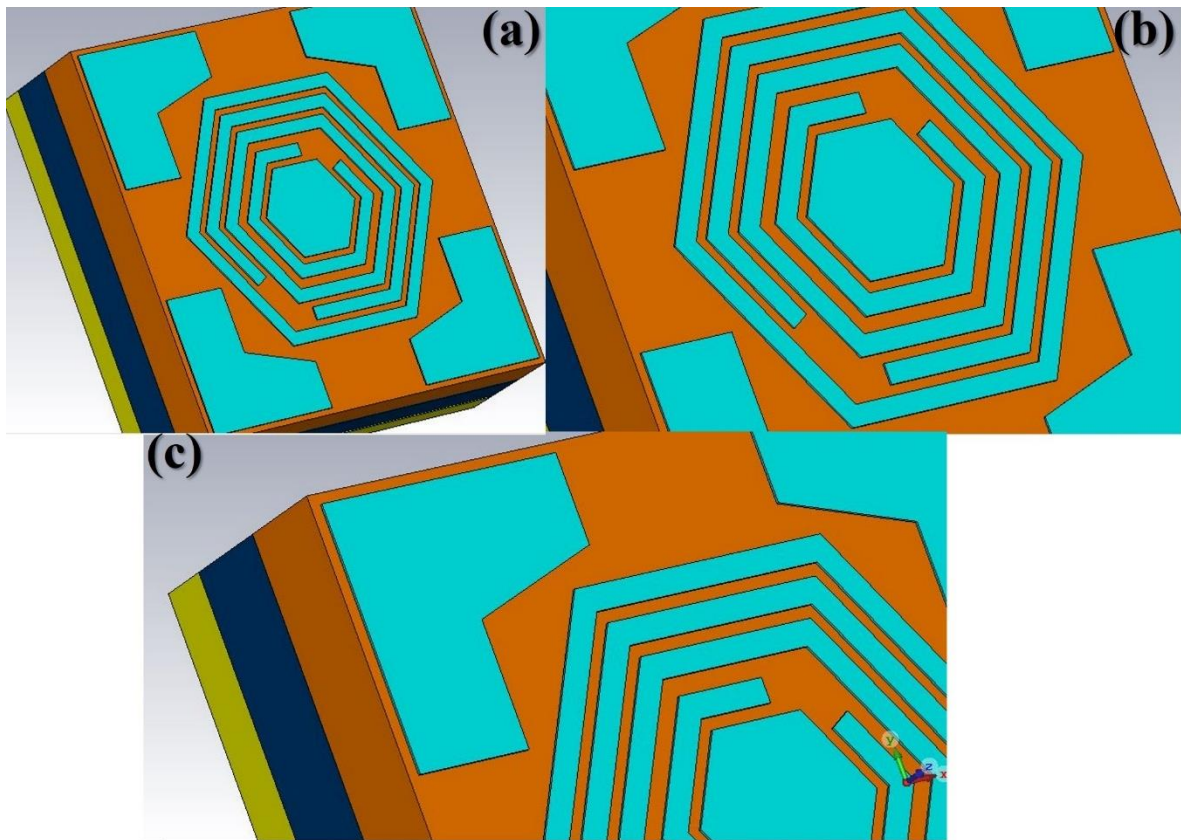


Figure S1: Designing details of the absorber. Image (a) hexagonal centroid and four annular hexagons surrounded with L-shaped corner elements, (b) rings with split positioned oppositely in the first and third ring, (c) orientation of hexagon with corner elements.

Figure S1 shows more detail view of FSS layer in which closed hexagon is surrounded with four rings. Image (a) shows orientation of hexagonal cluster with respect to the L-shaped corner elements. Image (b) shows nature of designed structure indicating split in every alternate ring. The split is at the opposite side. Image (c) shows orientation of hexagons with the corner elements. The corners of the hexagons are aligned with corner element for at the middle of the cell.

Table S1: Comparison of IFSS with recently reported structures.

Ref.	Unit cell (mm)	Thickness mm (λ_L)	BW (10 dB) GHz	FBW (%)	Angular stability	Polarisation Insensitivity	Type
[17]	17.6 \times 17.6	11.25 (0.075)	2.0–11.0	132.00	45 ⁰	No data	Lumped
[19]	15.5 \times 15.5	3.0(0.082)	8.2-13.4	51.16	65 ⁰	90 ⁰	Lumped
[21]	13.0 \times 13.0	5.0(0.1)	6.0-14.0	80.00	40 ⁰	45 ⁰	Resistive ink
[23]	10.1 \times 10.1	2.5(0.067)	8.0-20.0	88.52	60 ⁰	No data	Resistive ink
[24]	16.0 \times 16.0	8.0(0.08)	3.0-13.0	125.00	60 ⁰	45 ⁰	Resistive ink
[26]	16.0 \times 16.0	6.0(0.146)	6.0-16.0	90.00	No data	No data	Resistive ink
This work	10.6 \times 10.6	1.9(0.05)	8.0-18.0	77.00	60 ⁰	90 ⁰	Resistive ink

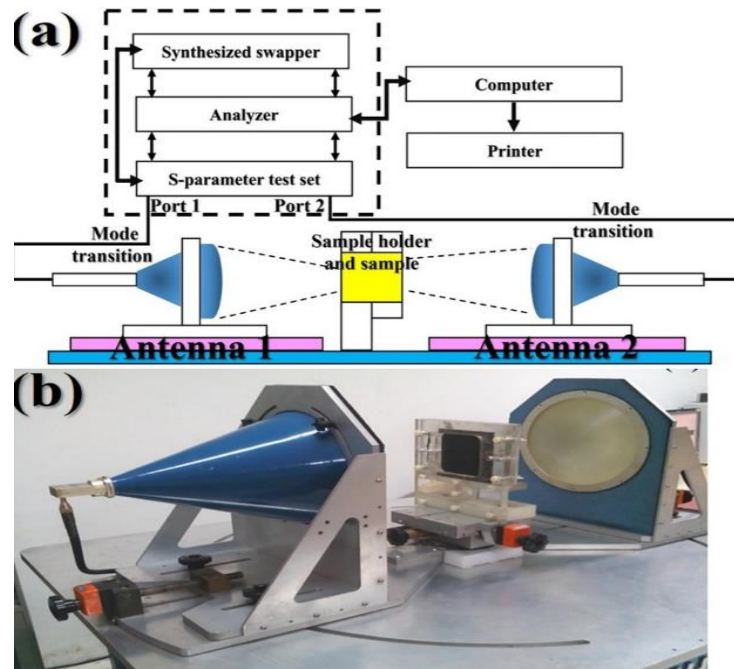


Figure S2: (a) Schematic layout of free space measurement system (FSMS) comprised of horn-shaped emitting (Antenna-1) and receiving (Antenna-2) port equipped with sample holder facility. The system is connected to the network analyser in a serial port configuration. Various modules of network analyser like scattering parameter module, frequency analyser, and frequency sweeper is shown with a dashed box connected to the output (PC/printable media) of the system.

Figure S2(a) provided in supporting information displays shows schematic block diagram schematic and actual setup of FSMS, which consists of pair of focusing transmitting and

receiving horn lens antennas, sample holder and a vector network analyser. The vector network analyser (VNA) has a scattering parameter module, frequency sweeper and analyser unit, it is also equipped with a computer and printing medium. Figure 2(b) shows the spot focusing horn lens antenna consists of two equal plano-convex dielectric lens mounted back-to-back in order to focus the incident electromagnetic power at a focal length of 30.5 cm. The laminates were placed on sample holder which was positioned at the common focal plane of the antennae, *Through-Reflect-Line* (TRL) calibration has been carried out before performing the constitutive measurements in order to avoid systematic errors. Finally, transmission and reflection measurements were performed to obtain dielectric properties of test specimens.

Figure S3(a) shows linear variations in reflection loss values under TE mode as a function of incidence angle (θ). The observed variation is an indication for robust angular stability of proposed absorber. Figure S3(b) data underlines the dispersive behaviour of the absorber recorded for TM mode. Nevertheless, simulated absorber has a commensurate angular stability for TM as well as TE mode. By and large, TM analysis showed an offset magnetic polarization in IFSS absorber with respect to TE polarization.

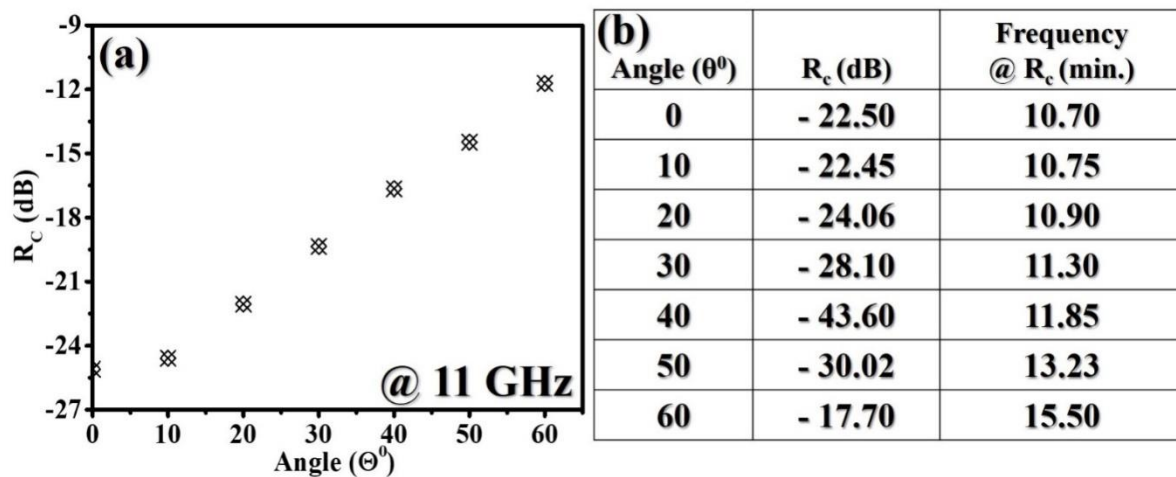


Figure S3:(a) Depicts variation in R_c corresponding to 11 GHz for TE mode, (b) data representing dispersive behaviour of TM mode for the absorber.

Analysis of simulated displacement current distribution for TM mode: front vs back surface

Similar analysis for the surface current distribution has been carried for TM mode, it can be observed that magnetic coupling is more prominent under this situation. The front surface current distribution has been shown in Figure S4(a) and (c), respectively corresponding to incidence angle of 0° and 60° respectively. The corresponding rear part of current distribution is shown in Figure S4(b) and (d). The discussion on engaging TM mode by the absorber is analogous to that of TE mode. The difference is seen in the direction of the current vector with respect to TE mode.

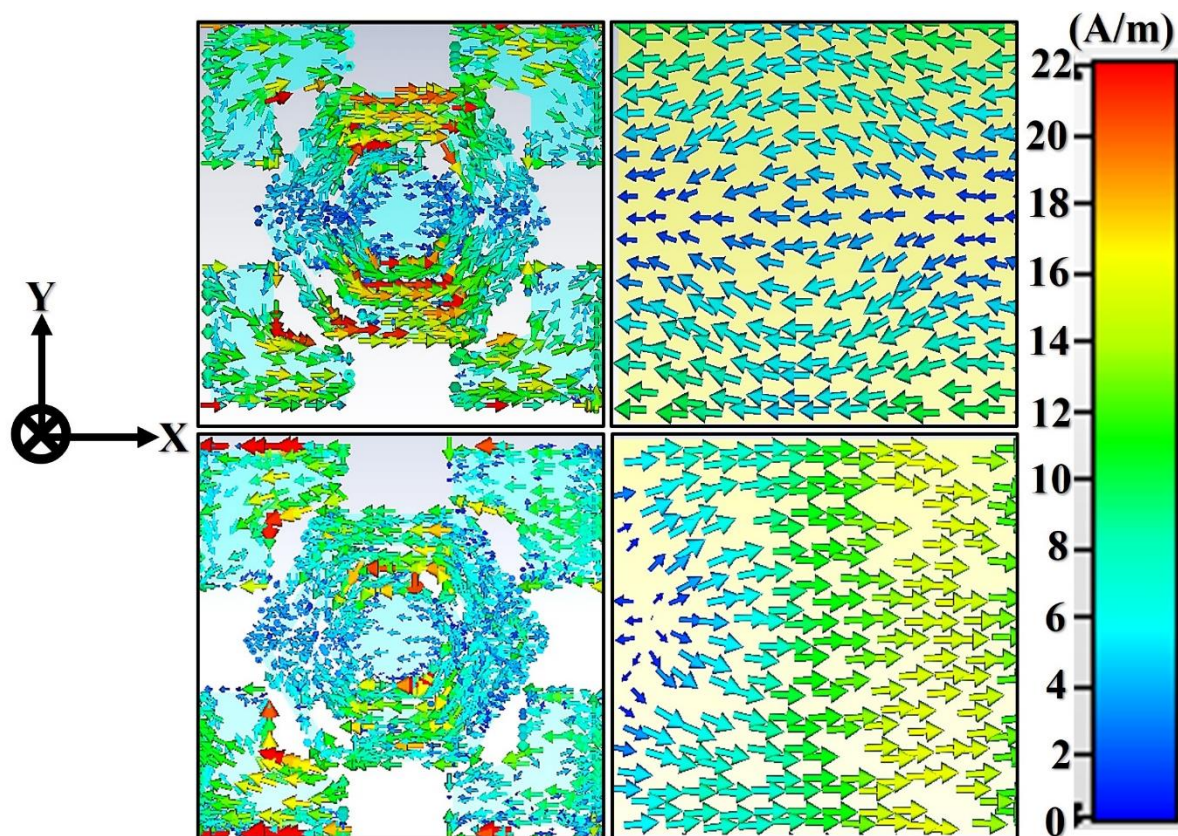


Figure S4: Simulated mode TM surface current profiles at 11 GHz. Plots (a) and (c), respectively, front surface current topology for 0° and 60° and, correspondingly, plots (b) and (d) rear surface current distribution.

Physicochemical aspects of the resistive ink

In the current work, the customized resistive ink used for validation of simulated IFSS result has not been changed for its chemical composition, content, ratio and proportion. All materials that used as an ingredient of ink were CB, graphite (bulk), epoxy/polymer, etc., has been fixed for a sheet resistance value of $110 \Omega/\square$ obtained from the simulated result discussed in Figure 2. Hence, sheet resistance of the resistive ink was a crucial parameter and not the material composition. However, for the ready reference, following analysis of the ink material has been appended in Supporting Information as Figure S5.

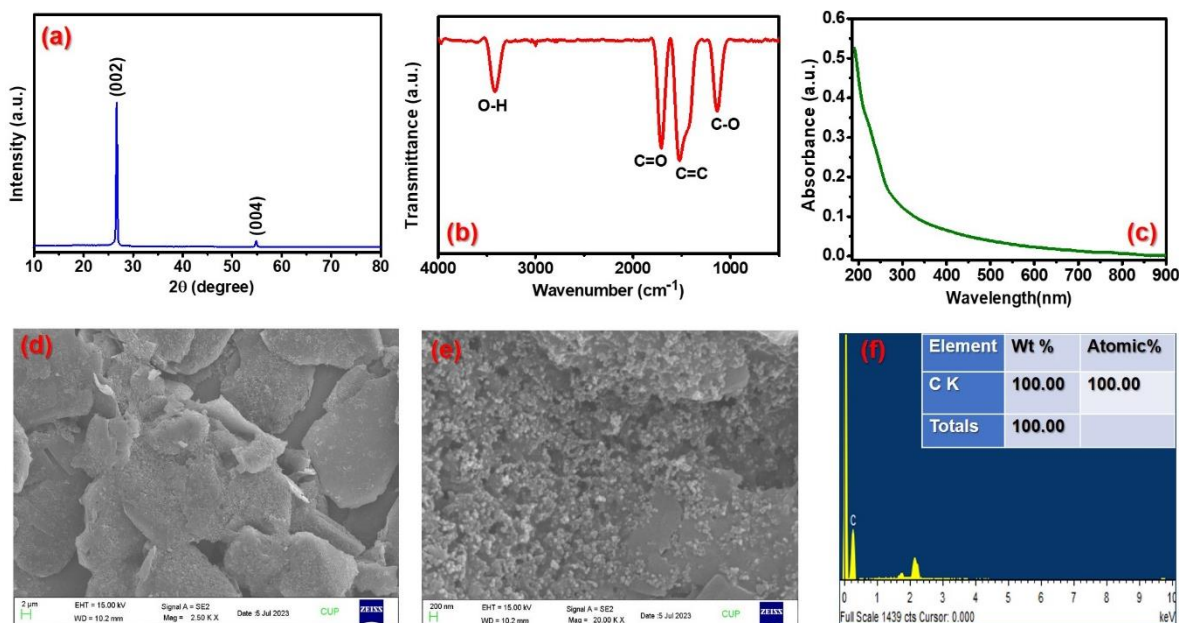


Figure S5: Recorded (a) XRD pattern, (b) Fourier Transform Infrared (FTIR) spectrum, (c) UV-Visible spectrum, and (d)-(e) typical Field emission scanning electron microscope (FESEM) images recorded at different magnifications (Scale bar: 1 μ m and 200 nm), and (f) EDX spectrum recorded for elemental composition of customized resistive ink used for FSS imprinting.

XRD pattern recorded for resistive ink is displayed in Figure S5 (a). The emergence of diffraction peak at $2\theta = 26.5^\circ$ and 54.5° corresponds to the Miller planes (002) and (004), respectively. These planes are attributed to typical graphitic sp^2 hybridized carbon layers and their inter layer spacing. The recorded FTIR spectrum in plot (b) indicate characteristics functional groups appeared at wave number 1110, 1570, 1695, and 3410 cm^{-1} which corresponds to C-O, C=C, C=O, and O-H, respectively. The presence of oxygen and hydroxyl group is indicative of donor loaded functional group that can readily participate to disperse well in host polymer/ epoxy matrix to form ink. Figure S5 (c) displays recorded UV-Visible absorption spectrum for resistive ink. By and large it shows the absorption edge at low wavelength region. The typical FESEM images recorded for the ink are shown in Figure S5 (d)-(e). The morphology of the material seems to be planner. The scaffolds of the graphitic contain are seen in the recorded images. They represent a characteristics morphology of the graphite. At some places coagulations of graphitic layers are prominently observed. The EDX spectrum recorded for the resistive ink is displayed in plot (d). It shows the dominant contribution from the elemental carbon that has come from graphitic carbon and host polymer. The atomic and weight % confirm the composition of carbon in the ink sample.